

FUNCTION

Right Ventricular Wall Motion Abnormalities Found in Healthy Subjects by Cardiovascular Magnetic Resonance Imaging and Characterized with a New Segmental Model

Burkhard Sievers, M.D.,* Marvin Addo, Ulrich Franken, M.D.,
and Hans-Joachim Trappe, M.D.

Department of Cardiology and Angiology, University of Bochum, Herne, Germany

ABSTRACT

Aim. To evaluate right ventricular wall motion abnormalities in healthy subjects using a new segmental model for the right ventricle. *Methods and Results.* 29 healthy subjects (9 female, 20 male, mean age 48.9 ± 15 years) underwent cardiovascular magnetic resonance imaging (CMR; 1.5-Tesla Sonata, Siemens, Erlangen, Germany) for the evaluation of cardiac function and right ventricular wall motion. A steady-state free precession gradient-echo sequence (TrueFISP) was used. Right ventricular wall motion was analyzed, and the site of areas of disordered motion was classified according to the new segmental model. Such areas were seen in 27 (93.1%) of the 29 subjects. Dyskinesia was found in 22 subjects (75.9%), hypokinesia in 11 (37.9%), and bulging in 8 (27.6%). The number of wall motion abnormalities diagnosed was significantly higher in the transverse plane (86.2%) than in the short-axis plane (13.8%) and the horizontal longitudinal plane (41.4%; $p = 0.000$). *Conclusion.* Right ventricular wall motion abnormalities are one of the criteria for the diagnosis of arrhythmogenic right ventricular cardiomyopathy. However, our findings indicate that they may also be seen around the insertion of the moderator band in healthy subjects, so that the significance of their presence at this site in patients undergoing diagnostic investigations for this disease should be interpreted with caution.

Key Words: Cardiac magnetic resonance imaging; Steady-state free precession gradient-echo sequence (TrueFISP); Right ventricular wall motion abnormalities; Right ventricular segmental model; Arrhythmogenic right ventricular cardiomyopathy.

*Correspondence: Burkhard Sievers, M.D., Duke Cardiovascular Magnetic Resonance Center, Duke University Medical Center, Duke Clinic, RM 00354, SB, Orange Zone/Trent Drive, DUMC 3934, Durham, NC 27710, USA; Fax: (919) 668-5588; E-mail: burkhard.sievers@gmx.de.

INTRODUCTION

Cardiovascular magnetic resonance imaging (CMR) allows accurate and reproducible evaluation of right and left ventricular function, volumes, and ejection fractions (Mackey et al., 1990; Mogelvang et al., 1986, 1988; Pattynama et al., 1995; Sakuma et al., 1993; van Rossum et al., 1988). Multiplane image acquisition makes CMR superior to other imaging techniques, especially for the examination of the right ventricle.

With the introduction of enhanced gradient-echo sequences, CMR can now produce precise images of right ventricular wall motion abnormalities that have not been visible before. The CMR requires only a short breath-holding period and offers high spatial and temporal resolution, which results in excellent blood-myocardium contrast and allows differentiation not only of the endocardium and epicardium but also of the trabeculae and muscular bands. The value of CMR in the diagnosis of arrhythmogenic right ventricular cardiomyopathy (ARVC) is well documented (Auffermann et al., 1993; McKenna et al., 1994; Midiri and Finazzo, 2001; Sommer et al., 1998; van der Wall et al., 2000). One of the criteria for the diagnosis of ARVC is the finding of right ventricular wall motion abnormalities (Corrado et al., 2000; McKenna et al., 1994; Midiri and Finazzo, 2001; Sommer et al., 1998).

A standardized segmental model would facilitate the classification of ventricular wall motion abnormalities and would be especially useful in the evaluation of disease progression, but no standardized model for the right ventricle is yet in common use. To our knowledge, it is not known whether right ventricular wall motion disorders are found in healthy subjects. To test the hypothesis that they are, we examined 29 healthy subjects referred to our hospital for routine cardiac investigation by CMR, using a segmental model that we developed for this purpose (Fig. 1).

METHODS

Subjects

A total of 29 healthy subjects (9 female, 20 male, age range 16–74 years, mean age 48.9 ± 15 years) were examined by CMR to evaluate cardiac function and identify possible right ventricular wall motion disorders. Demographic data are given in Table 1. The subjects included in the study had been referred to our hospital for routine cardiac investigation. All subjects were shown to be free of heart disease by noninvasive investigations (12-lead electrocardiogram, Holter-ECG, chest x-ray, treadmill exercise test, echocardiography). Five subjects could not undergo treadmill exercise

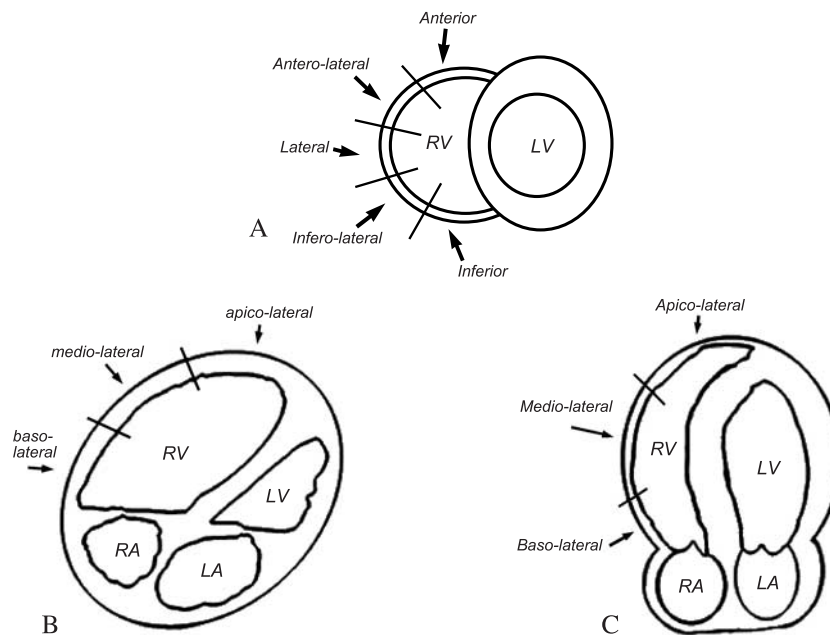


Figure 1. Segmental model for the right ventricle in the short-axis plane (A), transverse plane (B), and horizontal longitudinal plane (C) with wall segments marked.



Table 1. Demographic data of the subjects included in the study.

Age/yr	<i>n</i>	Min	Max	Mean±SD
Female	9	16	65	46.7±16.4
Male	20	25	74	49.9±14.7
Total	29	16	74	48.9±15

testing because of arthritis of the knees or hips; stress thallium scintigraphy with adenosine was performed instead.

The CMR showed the right ventricular outflow tract to be of normal size (mean diameter 2.3 ± 0.4 cm, measured in the transverse plane) and the right and left ventricular volumes and ejection fractions to be within the normal range in all the subjects (LV: EDV 102.9 ± 28.9 mL, ESV 29.2 ± 12.9 mL, SV 73.8 ± 20.8 mL, EF $72.1\% \pm 7.8\%$; RV: EDV 110.4 ± 33.7 mL, ESV 40.1 ± 15.7 mL, SV 70.1 ± 19.9 mL, EF $64.2\% \pm 6.3\%$). Fatty infiltration in the right and left ventricles was excluded by two experienced examiners (BS, MA, referred to as observer 1 and observer 2, respectively) using turbo spin echo sequences ($\kappa = 1.0$).

Arrhythmogenic right ventricular cardiomyopathy was not suspected in any of the subjects. None had a history of hypertension, myocardial infarction, arrhythmia, syncope, or a family history of ARVC. Physical examination was normal in all subjects.

Informed consent was obtained from all subjects before CMR. The study was conducted according to the principles of the Declaration of Helsinki. Approval of the institutional Review Board was not considered necessary, as the investigations are performed routinely in our department. Because they were clinically indicated in all the subjects, they would have been conducted even if the study had not been performed.

Image Acquisition

The CMR was performed with a 1.5-T Sonata (Magnetom, Siemens, Erlangen, Germany) using a front and rear surface coil (CP Body Array Flex, CP Spine Array, Siemens) and prospective electrocardiographic triggering. The anterior body array and the posterior spine array coil together give a four-element array combination. The dimensions of the coil elements are about 160 mm in the z-direction (head to feed) and about 460 mm in the x-direction (right to left). A fast imaging sequence with steady-state free precession (TrueFISP) and constant radiofrequency pulsing was used.

Short-axis, horizontal long-axis, and transverse cine-images were acquired on the basis of scout images. Short-axis and transverse scans were obtained with a breath-holding technique in end-expiration from the atrioventricular ring to the apex, with a 7-mm slice thickness and 3-mm interslice gap. The number of cardiac phases per image acquisition totaled 80%–90% of the R-R interval divided by the temporal resolution (TrueFISP: 43 ms). Seven to 11 slices were necessary to cover the complete right and left ventricle. The following parameters were used for TrueFISP: repetition time = 3.2 ms, echo time = 1.6 ms, slice thickness = 10 mm, flip angle = 60° , in-plane pixel size = 2.3×1.4 mm, matrix 164×256 pixel, trigger pulse 1, trigger delay 0, acquisition time = 12 heartbeats, breathhold duration per slice = 9–12 sec, depending on the heart rate.

Turbo spin echo images for ventricular tissue characterization were acquired with and without a preparation pulse for fat suppression using the same planes and slices as for the gradient-echo images and the following parameters: repetition time = 700 ms, echo time = 6.9 ms, slice thickness = 10 mm, flip angle = 180° , in-plane pixel size = 1.8×1.4 mm, matrix 166×256 pixel, trigger pulse 1, trigger delay 0 (dark blood preparation), acquisition time = 12 heartbeats, breathhold duration per slice = 7–10 sec, depending on the heart rate.

Prospective triggering with active ECG electrodes was used for both the TrueFISP and turbo spin echo sequences.

Image Analysis

Images were evaluated with conventional software (Argus, Siemens, Erlangen, Germany) by both observers, who were each unaware of the findings of the other. All images were of good quality and could be analyzed. For right ventricular wall motion assessment, the images were displayed in the cine modus in each section plane. Areas of disordered right ventricular wall motion were evaluated and classified with the help of a standardized segmental model for the right ventricle that had been developed by the authors (Fig. 1). The right ventricle is divided into 11 segments, which are evaluated in three planes (short axis, transverse, and horizontal longitudinal plane) in each subject. The segments were defined with reference to the model already established for the left ventricle (Cerqueira et al., 2002). A total of 319 segments were evaluated. Wall motion abnormalities were classified as akinesia, hypokinesia, dyskinesia (in ventricular systole), and bulging (in ventricular

diastole). The slices of the various section planes that showed wall motion abnormalities were counted.

The length of the involved part of the wall was marked in each slice with a cursor and measured by using a conventional software program (Siemens). The right ventricular outflow tract was evaluated in the transverse plane.

Statistical Analysis

Absolute and relative frequencies were determined for the categorical variables. The mean and standard deviation were derived for the right and left ventricular volumes and ejection fractions. For the diameter of the affected areas, the mean and standard deviation, median, minimum, and maximum values were determined. Fisher's exact test was used to examine the dependency of two categorical variables. Nonparametric tests were used to compare two or more groups with respect to a numerical variable. To compare two groups, the Mann-Whitney U-test was used. To compare more than two groups, the Kruskal-Wallis test was used. The significance level was set at 0.05 for all the tests. The kappa-statistic was used to quantify interobserver agreement with regard to categorical variables. For the diameter of the areas of disordered motion and the interobserver differences in the measurements, the mean and standard deviation, minimum, and maximum were determined. The Wilcoxon signed rank test was used to test the null hypothesis that both distributions were equal.

RESULTS

Turbo spin echo images did not reveal fatty infiltration in the right or left ventricular myocardium in any of the subjects included in the study.

Table 2. Wall motion abnormalities: interobserver agreement.

	Kappa
Location on the basis of the segmental model	0.95
Type (dyskinesia, hypokinesia, bulging)	0.95
Location in relation to moderator band	0.97
Number of slices in which present	1.0
Location with reference to slice level (basal, midventricular, apical)	0.97

Table 3. Comparison of the values obtained for the diameter of the right ventricular wall motion abnormalities (cm) between the two observers.

	Mean ± SD (min–max)	<i>p</i> Value ^a
Observer 1	0.60 ± 0.7 (0–3)	0.1505
Observer 2	0.63 ± 0.7 (0–3)	
Difference (obs. 1 – obs. 2)	–0.03 ± 0.19 (0–3)	—

^aWilcoxon signed rank test.

Interobserver agreement is shown in Table 2. The measurements for the diameter of the areas of disordered motion did not differ significantly between the two observers (Table 3).

The numbers of subjects with wall motion abnormalities/disorders, the segments affected, and their relation to the insertion of the moderator band and/or trabeculae as detected in the various section planes are given in Table 4 and Fig. 2.

Examination of all three section planes revealed a total of 56 right ventricular wall motion abnormalities spread over 95 (29.8%) of the 319 segments. Dyskinesia was found in 22 subjects (75.9%), hypokinesia in 11 (37.9%), and bulging in 8 (27.6%). Akinesia was not found. Two subjects (6.9%) exhibited no right ventricular wall motion abnormalities. A single segment was affected in 14 subjects (48.3%), two segments in 11 subjects (37.9%), and three segments in two subjects (6.9%). The number of wall motion abnormalities detected in the transverse plane (86.2%) was significantly higher than in the short-axis plane (13.8%) and the horizontal longitudinal plane (41.4%); *p* = 0.000; Table 4). In 7 subjects (24.1%), no relation to the insertion of the moderator band or trabeculae was noted. However, most wall motion abnormalities were located to the right of (51.2%) or between (48.3%) the insertions of the moderator band (Table 5). Among those located to the right of the insertions, dyskinesia was found significantly more often than hypokinesia or bulging (*p* = 0.002; Fig. 3). Among those observed between the insertions of the moderator band, hypokinesia was seen significantly more often than the other types (*p* = 0.000; Table 5). The number of slices with wall motion “abnormalities” was independent of the section plane (*p* = 0.862). The diameter of the wall motion abnormalities differed significantly among the various planes (*p* = 0.0140; Table 6).

Table 4. Incidence of right ventricular wall motion “abnormalities” in the various planes according to the segment involved, type, and relation to the insertion of the moderator band/trabeculae.

Findings	Transverse		Short axis		Horizontal long axis	
	<i>n</i>	%	<i>n</i>	%	<i>n</i>	%
N=29 (100%)						
<i>Segment affected</i>						
Apicolateral	23	79.3	–	–	10	34.5
Mediolateral	10	34.5	–	–	5	17.2
Basolateral	–	–	–	–	–	–
Inferolateral	–	–	4	13.8	–	–
Wall motion abnormality	25	86.2	4	13.8	12	41.4
Dyskinesia	19	65.5	–	–	9	31.0
Hypokinesia	9	31.0	–	–	3	10.3
Bulging	2	6.9	4	13.8	3	10.3
<i>Relation to insertion</i>						
To right	14	48.3	–	–	3	10.3
To left	6	20.7	–	–	3	10.3
Between branches	2	6.9	2	6.9	4	13.8
Above	9	31.0	–	–	4	13.8
No relation	2	6.9	2	6.9	3	10.3

DISCUSSION

The results of this study indicate that areas of disordered motion may be seen in the right ventricular wall in healthy subjects with no diagnostic criteria for ARVC. Such “abnormalities” were found by CMR in 93.1% of the subjects investigated and were mostly located around the area of insertion of the moderator band and trabeculae (Figs. 4 and 5). However, the extent of the wall motion “abnormalities” we found in subjects without cardiac disease was small (Table 6), and the regions of wall motion abnormalities are likely to result from tethering of the free wall by the

moderator band. Because the moderator band inserts mediolaterally to apicolaterally on the free wall of the right ventricle, it is mainly those wall sections that are of relevance for the diagnosis of ARVC that are affected. It is possible that through-plane motion effects resulting from the substantial long-axis contraction of the right ventricle during ventricular systole may have contributed to the high prevalence of right ventricular wall motion abnormalities noted in healthy subjects in this study.

The CMR allows accurate and reproducible evaluation of cardiac function and right and left ventricular volumes and ejection fractions (Lorenz et al., 1999; Mackey et al., 1990; Mogelvang et al., 1986, 1988; Pattynama et al., 1995; Sakuma et al.,

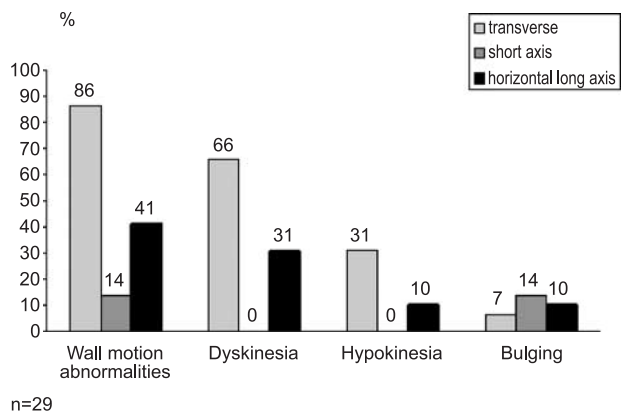


Figure 2. Frequency of wall motion “abnormalities” in the various different section planes.

Table 5. Incidence of the various types of wall motion “abnormalities” in relation to the insertion of the moderator band.

Relation to insertion	Dyskinesia (%)	Hypokinesia (%)	Bulging (%)
To right (<i>n</i> = 20)	18 (90)	2 (10)	0 (0)
To left (<i>n</i> = 9)	7 (78)	0 (0)	2 (22)
Above (<i>n</i> = 6)	5 (83)	0 (0)	1 (17)
Between branches (<i>n</i> = 14)	3 (19)	10 (62)	3 (19)
No relation (<i>n</i> = 7)	3 (43)	1 (14)	3 (43)

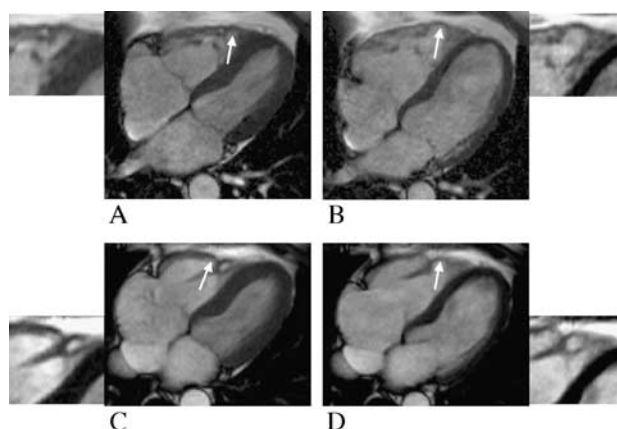


Figure 3. Sample images of right ventricular wall motion “abnormalities” acquired with gradient echo cine sequence TrueFISP in the horizontal longitudinal plane (A, B), and transverse plane (C, D) and in detail. Dyskinesia (arrow in A) can be seen to the right of the insertion of the moderator band in ventricular systole. Figures B and D (both taken in ventricular diastole) show apicolateral to lateral bulging between the muscular insertions (arrows). In C (ventricular systole), hypokinesia can be seen to the left of the insertion of the moderator band (arrow).

1993; van Rossum et al., 1988). Because it offers multiplane imaging, excellent visualization of the right ventricle can be obtained (Dehmer et al., 1982; Doberty et al., 1992; Lorenz et al., 1995; Ohsuzu et al., 1980; Pattynama et al., 1995; Pietras et al., 1983). The CMR is an important tool in the diagnosis of ARVC, its capability for tissue characterization and right ventricular wall motion evaluation being of particular importance. Previous studies were performed with machines of lower gradient power (0.5 T) and older spin echo or gradient echo sequences (Auffermann et al., 1993; Sommer et al., 1998; van der Wall et al., 2000) that did not enable such clear distinction of blood, myocardium, and the insertion of the mod-

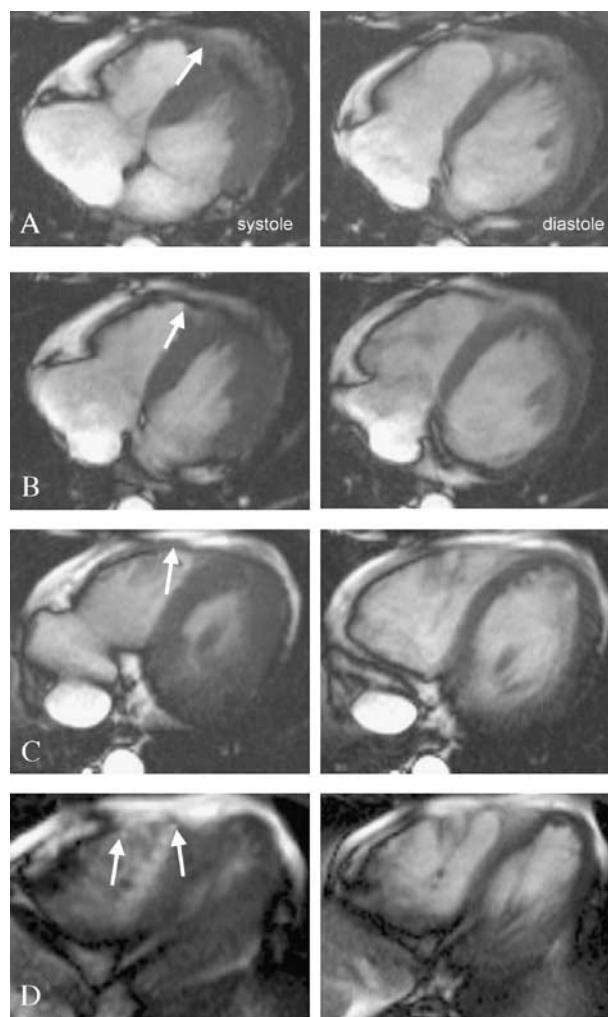


Figure 4. Transverse slices through the right ventricle from the base mid-ventricular borderline to the apex (left: ventricular systole; right: ventricular diastole). An area of hypokinesia can be seen to the right of the moderator band insertion (A, arrow) in the apicolateral segment; above the insertion there are areas of hypokinesia (B) and dyskinesia (C); hypokinesia is seen to the left of the insertion (arrow). Figure D shows dyskinesia to the right of the insertion (arrow).

Table 6. Values relating to the diameter of the wall motion “abnormalities” in the three individual planes.

Section plane	N	Min	25th Percentile	Median	75th Percentile	Max	Mean	SD
Transverse	36	0.2	0.65	0.90	1.05	2.7	0.98	0.54
Short axis	4	1.3	1.3	1.4	1.9	2.3	1.58	0.49
Horizontal long axis	15	0.70	0.90	1.2	1.4	3	1.3	0.64

Diameter of wall motion abnormalities/cm.

Kruskal-Wallis test: $p = 0.0140$.

Minimum diameters were found in the transverse section plane (0.9 ± 0.54 cm; $n = 36$).

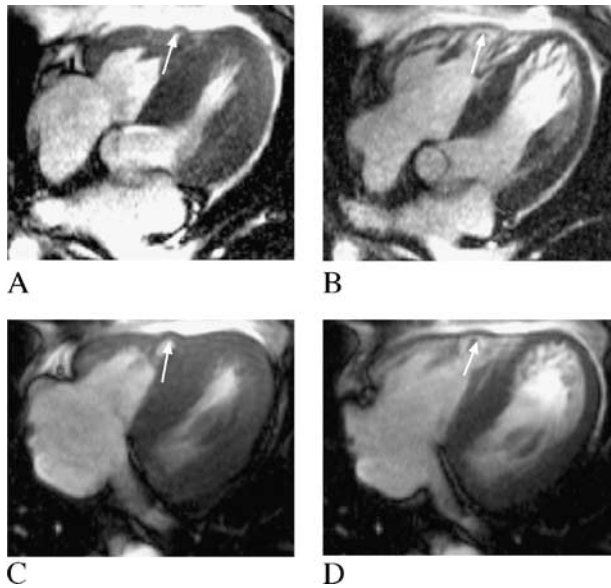


Figure 5. Horizontal longitudinal plane (A, B) with dyskinesia (arrow in A) to the right of the moderator band insertion (A, ventricular systole) and bulging (arrow in B) in the apicolateral/lateral segment in ventricular diastole. In the transverse plane (C, D), dyskinesia was found to the right of the moderator band insertion (arrow in C, ventricular systole). Figure D (ventricular diastole) shows bulging (arrow) between the two branches of the forked moderator band insertion.

erator band and trabeculae on the ventricular wall as more recently developed gradient-echo sequences with steady-state free precession (TrueFISP). The latter are able to detect previously unnoticed right ventricular wall motion abnormalities that are not necessarily of any clinical relevance. Thus, it is now important to distinguish nonpathological wall motion disorders from pathological wall motion abnormalities to prevent an incorrect diagnosis from being made.

Echocardiography is widely available and is the most commonly used first-line method of cardiac imaging in the investigation of patients with suspected heart disease. However, it is of limited value in the diagnosis of ARVC because it only allows assessment for right ventricular wall motion abnormalities and right ventricular dilatation, and even this is not always possible because the image quality is often poor (Kisslo, 1989; Moro et al., 1987; Robertson et al., 1985; Yoshioka et al., 2000). Additional evaluation of the right ventricular outflow tract is possible if right ventricular catheter angiography is performed (Auffermann et al., 1993; Robertson et al., 1985). Because of its higher spatial and temporal resolution, CMR is superior to both these procedures, especially when it

comes to detailed evaluation and classification of right ventricular wall motion abnormalities and the identification of small, locally restricted abnormalities. Multiplane CMR is currently the most effective tool for the noninvasive diagnosis of ARVC (Auffermann et al., 1993; Sommer et al., 1998; van der Wall et al., 2000). With spin echo sequences, tissue characterization is possible and fat can be identified. The diagnosis of ARVC has to be based in part on the subject's medical history and electrocardiographic and electrophysiological findings, as well as the histopathological findings (McKenna et al., 1994).

Because it is often very difficult to differentiate normal from pathological CMR findings, we recommend that interpretation should be performed by well-experienced examiners. The fact that right ventricular wall motion abnormalities may also be seen in healthy subjects is of relevance for the evaluation of screening tests, and awareness of this may help to prevent the misinterpretation of findings.

The segmental model for the right ventricle that we developed for this study could be used as a basis for standardization of the findings of further studies and of investigations in clinical practice, facilitating the comparison of the results of follow-up examinations.

REFERENCES

- Auffermann, W., Wichter, T., Breithardt, G., Joachimsen, K., Peters, P. E. (1993). Arrhythmogenic right ventricular disease: MR imaging vs. angiography. *AJR* 161:549–555.
- Cerqueira, M. D., Weissman, N. J., Dilsizian, V., Jacobs, A. K., Kaul, S., Laskey, W. K., Pennell, D. J., Rumberger, J. A., Ryan, T., Verani, M. S. (2002). Standardized myocardial segmentation and nomenclature for tomographic imaging of the heart: a statement for healthcare professionals from the cardiac imaging committee of the council on clinical cardiology of the American heart association. *Circulation* 105:539–542.
- Corrado, D., Fontaine, G., Marcus, F. I., McKenna, W. J., Nava, A., Thiene, G., Wichter, T. (2000). Arrhythmogenic right ventricular dysplasia/cardiomyopathy: need for an international registry. *J. Cardiovasc. Electrophysiol.* 7:827–831.
- Dehmer, G. J., Firth, B. G., Hillis, L. D., Nicod, P., Willerson, J. T., Lewis, S. E. (1982). Nongeometric determination of right ventricular volumes from equilibrium blood pool scans. *Ann. J. Cardiol.* 49:79–84.
- Doherty, N. E. III., Fujita, N., Caputo, G. R., Higgins, C.



- B. (1992). Measurement of right ventricular mass in normal and dilated cardiomyopathic ventricles using cine magnetic resonance imaging. *Am. J. Cardiol.* 69:1223–1228.
- Kisslo, J. (1989). Two-dimensional echocardiography in arrhythmogenic right ventricular dysplasia. *Eur. Heart J.* 10(Suppl. D):22–26.
- Lorenz, C. H., Walker, E. S., Graham, T. P. Jr., Powers, T. A. (1995). Right ventricular performance and mass in adults late after atrial repair of transposition of the great arteries using cine magnetic resonance imaging. *Circulation* 92(Suppl. 11): 233–239.
- Lorenz, C. H., Walker, E. S., Morgan, V. L., Klein, S. S., Graham, T. P. Jr. (1999). Normal human right and left ventricular mass, systolic function, and gender differences by cine magnetic resonance imaging. *J. Cardiovasc. Magn. Reson.* 1:7–21.
- Mackey, E. S., Sandler, M. P., Campbell, R. M., Graham, T. P. Jr., Atkinson, J. B., Price, R., Moreau, G. A. (1990). Right ventricular myocardial mass quantification with magnetic resonance imaging. *Am. J. Cardiol.* 65:529–532.
- McKenna, W. J., Thiene, G., Nava, A., Fontaliran, F., Blomstrom-Lundqvist, C., Fontaine, G., Camerini, F. (1994). Diagnosis of arrhythmogenic right ventricular dysplasia/cardiomyopathy. *Br. Heart J.* 71:215–218.
- Midiri, M., Finazzo, M. (2001). MR Imaging of arrhythmogenic right ventricular dysplasia. *J. Cardiovasc. Imaging* 17:297–304.
- Mogelvang, J., Stubgaard, M., Thomsen, C., Henriksen, O. (1988). Evaluation of right ventricular volumes measured by magnetic resonance imaging. *Eur. Heart J.* 9:529–532.
- Mogelvang, J., Thomsen, C., Mehlsen, J., Brackle, G., Stubgaard, M., Henriksen, O. (1986). Evaluation of left ventricular volumes measured by magnetic resonance imaging. *Eur. Heart J.* 7:1016–1021.
- Moro, E., Pignoni, P., Nicolosi, G. L., Zardo, F., Burelli, C., Vergara, G., Furlanello, F., Zanuttini, D. (1987). Value and limitations of 2-dimensional echocardiography in the identification of arrhythmogenic right ventricular dysplasia. *G. Ital. Cardiol.* 17: 661–666.
- Ohsuzu, F., Handa, S., Kondo, M., Yamazaki, H., Tsugu, T., Kubo, A., Takagi, Y., Nakamura, Y. (1980). Thallium-201 myocardial imaging to evaluate right ventricular overloading. *Circulation* 61: 620–625.
- Pattynama, P. M., Lamb, H. J., Van der Velde, E. A., Van der Geest, R. J., van der Wall, E. E., De Roos, A. (1995). Reproducibility of magnetic resonance imaging-derived measurements of right ventricular volumes and myocardial mass. *Magn. Reson. Imaging* 13(1):53–63.
- Pietras, R. J., Kondos, G. T., Kaplan, D., Lam, W. (1983). Comparative angiographic right and left ventricular volumes. *Ann. Heart J.* 109:321–326.
- Robertson, J. H., Bardy, G. H., German, L. D., Gallagher, J. J., Kisslo, J. (1985). Comparison of two-dimensional echocardiographic and angiographic findings in arrhythmogenic right ventricular dysplasia. *Am. J. Cardiol.* 55:1506–1508.
- Sakuma, H., Fujita, N., Foo, T. K., Caputo, G. R., Nelson, S. J., Hartiala, J., Shimakawa, A., Higgins, C. B. (1993). Evaluation of left ventricular volume and mass with breath-hold cine MR imaging. *Radiology* 188:377.
- Sommer, T., Lewalter, T., Bierhoff, E., Pakos, E., von Smekal, A., Pauleit, D., Hofer, U., Luderitz, B., Schild, H. (1998). MRT-Diagnostik der rechtsventrikulären Dysplasie. *Fortschr. Röntgenstr.* 169: 609–615.
- van der Wall, E. E., Kayser, H. W., Bootsma, M. M., de Roos, A., Schalij, M. J. (2000). Arrhythmogenic right ventricular dysplasia: MRI findings. *Herz* 25:356–362.
- van Rossum, A. C., Visser, F. C., van Eenige, M. J., Valk, J., Roos, J. P. (1988). Magnetic resonance imaging of the heart for determination of ejection fraction. *Int. J. Cardiol.* 18:53–63.
- Yoshioka, N., Tsuchihashi, K., Yuda, S., Hashimoto, A., Uno, K., Nakata, T., Shimamoto, K. (2000). Electrocardiographic and echocardiographic abnormalities in patients with arrhythmogenic right ventricular cardiomyopathy and in their pedigrees. *Am. J. Cardiol.* 85:885–889.



Request Permission or Order Reprints Instantly!

Interested in copying and sharing this article? In most cases, U.S. Copyright Law requires that you get permission from the article's rightsholder before using copyrighted content.

All information and materials found in this article, including but not limited to text, trademarks, patents, logos, graphics and images (the "Materials"), are the copyrighted works and other forms of intellectual property of Marcel Dekker, Inc., or its licensors. All rights not expressly granted are reserved.

Get permission to lawfully reproduce and distribute the Materials or order reprints quickly and painlessly. Simply click on the "Request Permission/Order Reprints" link below and follow the instructions. Visit the [U.S. Copyright Office](#) for information on Fair Use limitations of U.S. copyright law. Please refer to The Association of American Publishers' (AAP) website for guidelines on [Fair Use in the Classroom](#).

The Materials are for your personal use only and cannot be reformatted, reposted, resold or distributed by electronic means or otherwise without permission from Marcel Dekker, Inc. Marcel Dekker, Inc. grants you the limited right to display the Materials only on your personal computer or personal wireless device, and to copy and download single copies of such Materials provided that any copyright, trademark or other notice appearing on such Materials is also retained by, displayed, copied or downloaded as part of the Materials and is not removed or obscured, and provided you do not edit, modify, alter or enhance the Materials. Please refer to our [Website User Agreement](#) for more details.

[Request Permission/Order Reprints](#)

Reprints of this article can also be ordered at

<http://www.dekker.com/servlet/product/DOI/101081JCMR120038528>